SPE 29115

Evaluating Miscible and Immiscible Gas Injection in the Safah Field, Oman

Charles L. Hearn, *Occidental International Exploration and Production Co.*, and
Curtis H. Whitson, *U. Trondheim, Norwegian Institute of Technology*
SPE Members

This paper was prepared for presentation at the 13th Symposium on Reservoir Simulation in San Antonio, Texas, February 12-15, 1995.

Abstract

The reservoir modeling approach presented in this paper illustrates how available engineering tools can be used to evaluate the technical feasibility and economics of high-pressure gas injection. The key components to such a study included: 1) equation of state (EOS) modeling of experimental PVT data, matching miscible and immiscible slim tube results, and systematically reducing the number of components used in the EOS model to minimize computational requirements, 2) studying numerical grid effects, displacement mechanisms, optimal well pattern, and injection pressure with 2D cross-section and 3D sector models, and 3) comparing compositional results with simulations based on the black-oil PVT formulation used in full-field history matching and reservoir management modeling.

Introduction

Safah field, in northwest Oman, produces light oil from a low-permeability carbonate formation at 6500 ft. Produced gas is processed and the lean plant residue gas is reinjected at high pressure. Laboratory tests show that such injection can increase recovery by oil vaporization, swelling, and viscosity reduction, and that injecting a suitably enriched gas would develop miscibility. We used a PVT program, compositional model, and black-oil model to study these effects. The purposes of this paper are: 1) to illustrate the evaluation process, showing how simulation can extend laboratory results and determine displacement mechanisms; and 2) to show effects of operating variables such as gas enrichment, well pattern configuration, and injection pressure on Safah oil recovery.

References and illustrations at end of paper.

This paper focuses on the evaluation process, rather than on the performance of the present Safah gas injection project. Reservoir properties are summarized here; details of field geology, development, and operation are in previous papers.[1,2] Safah produces 42° API, low viscosity (0.4 cp) oil from a recrystallized lime mud. Original oil-in-place was about 650 MMSTB. The reservoir rock has been altered by complex diagenesis, which contributes to a reservoir structure that is not strongly layered. Safah reservoir pay has generally high porosity, but permeability averages only about 5 md. The field has variable oil properties with both saturated and undersaturated oil areas. This paper concerns evaluation of gas injection in the *undersaturated* oil area. The BHP of injection wells in this area is over 4000 psi, compared to an initial reservoir pressure of 3100 psia and oil bubblepoint pressure about 2100 psia. Reservoir and oil properties are summarized in Table 1.

Study Methods

On the basis of standard and multicontact gas injection PVT data, Safah oil was characterized with an EOS-based PVT program[3] using 15 components and the Peng-Robinson equation of state. Laboratory slim tube displacements using both lean and enriched gases were evaluated using a compositional simulator.[4] This included the determination of minimum miscibility pressure (MMP) and displacement mechanisms for the lean and rich injection gases.

The oil characterization was "pseudoized" to 8 components for compositional simulation. Cross-section model runs were used to compare the 15- and 8-component characterizations and to evaluate model grid-size effects. Finally, three-dimensional pattern simulations were conducted for lean and rich gas injection to evaluate such operating variables as pattern configuration and injection pressure. Compositional effects were isolated by parallel simulations using a two-component (black-oil) characterization.

PVT Evaluation and EOS Characterization

Heptanes-Plus Characterization. An EOS fluid characterization was developed using experimental PVT data which included TBP (true boiling point) analysis to describe the C_{7+} fractions of the reservoir oil, constant composition expansion and differential liberation at reservoir temperature, multi-stage separator data, and multi-contact gas injection studies.

The TBP data were characterized using a molar distribution model[5,6] and the Søreide specific gravity and boiling point correlations.[7] Critical properties were estimated using the Twu correlations.[7] With the experimental TBP data fit to C_{7+} characterization models, five "optimal" pseudocomponents were selected using Gaussian quadrature.[6] This method has the advantage that multiple fluids from the same reservoir (but with differing bulk C_{7+} properties) can be characterized with a *single* set of pseudocomponents. The properties of the pseudocomponents are the same for all fluids, but the mole fractions of pseudocomponents are different for each fluid. In this approach, *all* quality PVT data from *all* reservoir samples can be fit matched simultaneously with a single, consistent EOS model. In this study, ten fluid samples from six wells were included in the EOS characterization.

Tuning the Equation of State. PVT data were simulated using the Peng-Robinson EOS and the C_{7+} characterization described above. Slight adjustments were made to critical properties of the pseudocomponents, and binary interaction parameters between methane and pseudocomponents. Nonlinear regression was used to determine the parameter adjustments, where particular emphasis was placed on fitting compositional data from the multicontact gas injection tests, volumetric data from the differential liberation experiments, and separator test results. Some results of the EOS match are given in Fig. 1.

Two multicontact injection experiments were conducted with the lean gas, one at 3000 psig and the other at 4000 psig. The experiments were of the backward-contact type. First a specified amount of gas was injected to the original reservoir oil. The mixture was brought to equilibrium at the specified pressure (3000 or 4000 psig). All gas was removed and analyzed for composition. A small sample of oil was also analyzed. Physical properties such as density of the equilibrium gas and oil were measured and reported. More injection gas was then added to the remaining oil, and the process was repeated three times.

Careful analysis of the originally reported multicontact data (using material balance calculations) showed that an error had been made in the original reported PVT data. Without correction of this error, significant modifications of the original EOS characterization were needed to match the original (erroneous) results.

Reducing Number of Components ("Pseudoization"). The final 15-component EOS characterization was reduced to eight components for use in 3D pattern modeling studies. The "pseudoization" procedure ensured that the 8-component characterization replicated accurately the original 15-component characterization. This was achieved by (1) simulating numerous PVT experiments with the original characterization, (2) treating the calculated results as "data", (3) pseudoizing to eight components using the Coats procedure[14], (4) fine tuning the EOS parameters (EOS constants A and B for each pseudocomponent, and binary interaction parameters between methane and C_{7+} fractions) by nonlinear regression.

PVT experiments simulated with the original 15-component characterization included a differential liberation test, a multistage separator test, and four multicontact gas injection experiments (two with lean gas and two with rich gas) covering a pressure range from 2000 to 5000 psig. Calculated results were automatically stored as "data" that formed the basis for nonlinear regression in the pseudoization procedure.

The choice of pseudocomponents was based on a preliminary study using stage-wise application of the pseudoization procedure. Pseudoized characterizations with 12, 10, 8, and 6 pseudocomponents were developed. It was found that reducing from 8 to 6 pseudocomponents failed to replicate some of the key phase behavior of the original 15-component characterization. The final pseudoized characterization consisted of (C_1+N_2), (C_2+CO_2), C_{4s}, (C_{5s}+C_6), and three C_{7+} fractions (the heaviest with a molecular weight of 460). The final 15-component and 8-component EOS characterizations are given in Tables 2 to 4.

Slim Tube Data and Simulations. The lean injection gas represents a plant gas that is injected at Safah. The rich gas was determined from preliminary estimates of an enriched gas stream that could be generated from plant gas with a 30% solvent enrichment. This initial study did not try to optimize the enrichment level (i.e. determine the minimum miscibility enrichment, MME).

Slim tube measurements were made with the Safah oil and lean gas at 2500 and 4500 psig. Both tests showed immiscible displacements (49% and 89% recoveries at 1.2 PV injected). Significant vaporization occurred at the higher-pressure test. MMP was determined from the two tests to be about 5000 psig (±200 psi).

Rich gas slim tube experiments were run at 2500, 3500, and 4500 psig. Miscible displacements were indicated at 3500 and

4500 psig, with recoveries of 98% at 1.2 PV injected. A recovery of 84% was reported for the 2500 psig slim tube test; though clearly not miscible, this displacement had significantly greater recovery (through a near-miscible vaporization/condensation mechanism) than the lean-gas test at 2500 psig. The MMP estimated from the recovery-pressure curve is about 3300 psig for the rich gas. Fig. 2 shows the measured slim tube results for both lean- and rich-gas injection.

Slim tube simulations (1D) were made using the 15-component and 8-component EOS characterizations. Relative permeabilities were adjusted slightly to match the 2500 psig immiscible rich gas slim tube results. Calculated slim tube results matched the experimental data quite accurately, as shown in Fig. 3 for rich gas injection at 3500 psig.

Some numerical dispersion was observed in the slim tube simulations, as should be expected. Simulations using 100, 250, and 500 grids were compared. At a specific pressure, a plot of recovery at 1.2 PV injected versus inverse grid cell number ($x=1/N$ or $x=1/N^{0.5}$) was used to extrapolate to a dispersion-free recovery (where $x=0$). For this study, a model with 250 grids was used for most of the simulations. Dispersion-free recoveries were also determined.

PVT multi-contact calculations can also be used to estimate MMP (and MME). However, all published algorithms[10,11] predict MMP/MME for a strictly vaporizing mechanism (using a "static" or single-cell multicontact process). The condensing/vaporizing mechanism described by Zick[9] gives a more accurate description of most high-pressure gas displacements, and particularly if the injection gas has been enriched. Furthermore, if the condensing/vaporizing mechanism exists, it will *always* result in an MMP/MME that is less than the value predicted by the vaporizing mechanism.

An unpublished method has been developed by Zick[12] for accurately determining (defining) the MMP/MME for a condensing/vaporizing mechanism. A special interpretation of multi-cell contact calculations[13] is used, yielding MMP/MME estimates with high precision. This method was used to verify the dispersion-free MMPs estimated for rich-gas injection.

Table 5 presents results of MMP calculations for lean and rich gases with the Safah oil. The results are based on the vaporizing-only mechanism *and* the condensing/vaporizing mechanism. Dispersion-free slim tube results and measured MMPs are also given in the table. A vaporizing miscible mechanism is found for the lean gas injection, while the condensing/vaporizing mechanism develops for rich gas injection. Note the very large overprediction of MMP (1250 psi) for the rich gas assuming a vaporizing-only miscible drive mechanism.

A simple way to establish if a miscible slim tube simulation is encountering a vaporizing mechanism or the mixed condensing/vaporizing mechanism can be seen from a plot of gas/oil densities and oil saturation versus distance along the slim tube (prior to breakthrough, e.g. at 0.6 PV injected). Fig. 4(a) shows such a plot for the condensing/vaporizing rich-gas drive at the MMP of 3310 psig. Fig. 4(b) shows a similar plot for the rich-gas drive at a pressure equal to the vaporizing-mechanism MMP_{VM}=4525 psig (both results use the 15-component EOS characterization).

An "hour-glass" shape on the density-distance plot indicates a mixed condensing/vaporizing mechanism, with the miscible front being located at the minimum in density difference. Furthermore, two phases are found on *both* sides of the front. The extent of the two-phase region ahead of the front may vary from very short (for a highly undersaturated system) to quite long for a slightly-undersaturated (or initially two-phase) system.

A vaporizing-dominated process shows only the left side of the hour glass in the density-distance plot. Furthermore, a free gas saturation *can not* exist ahead of the front in a vaporizing mechanism, so two phases will only be found behind the front. Accordingly, the vaporizing mechanism can not develop miscibility in an initially saturated two-phase gas/oil system (unless reservoir pressure is increased sufficiently to redissolve all initial free gas).

Finally, a validity check of the 8-component EOS characterization was made by comparing 1D slim-tube and 2D cross-sectional simulations. Results are presented in Figs. 5-6, showing clearly that the 8-component characterization is accurate for lean- and rich-gas injection at pressures ranging from 2500 to 4500 psi.

Model Data and Controls

Model data used in cross-section and pattern simulation was based on reservoir properties in the Safah undersaturated oil area, typical injection and production well bottomhole pressures, and typical well spacing. Fig. 7 shows the vertical distribution of reservoir properties. Nine geologic zones have been mapped across the field based on log signatures. These are shown relative to the 173-ft total formation thickness and depths in the model area. Geologic zone average properties are in Table 6. The highest permeability (3-5 md) is in the upper part of the formation. Average vertical permeability is uncertain, but in Safah there are no correlatable tight zones in the upper part of the formation that could act as barriers to gas segregation. A K_v/K_h ratio of 0.5 was used in the models.

The initial vertical water/oil saturation distribution is shown on Fig. 7. The model capillary pressure curve, based on Safah well log S_w profiles, resulted in a 65-ft transition zone above the water-oil contact. In the 40-ft oil zone above the transition zone, initial oil saturation was 90%. The thick bottom water zone below the WOC provided a source of water production by water coning up to the model well perforations. Simulation runs used typical water-oil and gas-oil relative permeability curves. Residual oil saturation to both immiscible gas and water was 30%.

For better definition of gas displacement, the upper geologic zones were subdivided into thinner model layers. The lower zones below the WOC were combined into thick model layers. The 22 layers shown on Fig. 7, in which upper layers were about 4 ft thick (Table 6), were used for most model runs. Grid-size sensitivity runs were also made with 11, 33, and 44 model layers. In each case, model layers had the properties of their respective geologic zone.

Both injection and production wells were completed in the top two geologic zones (Fig. 7). Except for several runs in which sensitivity to injection pressure was investigated, injection was always at a constant bottomhole pressure of 4500 psig. Production wells were maintained at 1000 psig bottomhole pressure. Injection and production rates were not specified, but were controlled by the flowing bottomhole pressures. This causes injection and production rates to vary with time according to the ever-changing mobilities of the reservoir fluids and the fixed well indexes. This method of controlling gas injection corresponds to a possible future Safah project scenario in which additional gas is imported from nearby sources, with sufficient gas compression capacity always to inject at maximum injection well BHP. In this scenario, average reservoir pressure could be increased above initial reservoir pressure (3100 psig) depending on the ratio of injection to production wells.

Models were initialized at 2500 psig at a reference depth of 6010 ft subsea. Since this is above the bubblepoint pressure, there was no initial free gas. Both injection and production were started at time zero. Model runs were for 20 years, with continuous gas injection during this time. In the description of model runs to follow, the results are labeled according to three types of simulation:

- <u>EOS Model, Rich Gas Injection</u>—Simulation of rich gas (Table 2) displacing oil using the EOS compositional model.

- <u>EOS Model, Lean Gas Injection</u>—Simulation of lean plant residue gas (Table 2) displacing oil using the EOS compositional model.

- <u>Black-Oil Model</u>—Simulation of gas displacing oil using the compositional model run in 2-component, black-oil mode. Gas properties were those of lean plant residue gas. Standard black-oil properties for oil, including swelled oil due to gas injection, were generated by the PVT program based on the EOS characterization and field separation conditions.

The black-oil simulations are of interest since such models are used to help design and manage the present Safah field development.[1] Although black-oil models include the beneficial effects of oil swelling and viscosity reduction due to high-pressure lean gas injection, they do not account for compositional effects such as oil vaporization near injection wells. Comparison of the EOS model and the black-oil model predictions helps to separate the compositional effects from the other mechanisms.

Cross-Section Simulations

2D cross-section runs were made for three purposes: 1) to compare the 15- and 8-component fluid characterizations; 2) to study grid-size effects; and 3) to evaluate oil, gas, and water saturation distributions during gas injection. The cross-section model simulated one-quarter of a 5-spot injection pattern based on Safah average well spacing (62 acres per well). As shown on Fig. 8, the cross-section was variable width. This more accurately simulates reservoir flow velocities, which are high near wells and low in the interwell area. Gravity segregation, which is affected by flow velocity, is therefore modeled more realistically than in a constant width cross section. The ten x-direction grids shown were subdivided for runs with 20, 30, or 40 grids. Predicted oil recovery for the cross-section is higher than in 3D pattern runs since areal sweep efficiency is 100%.

Comparison of 8- and 15-Component Fluid Characterizations. Fig. 6 shows the cross-section production performance for lean and rich gas injection using the original 15-component and the pseudoized 8-component fluid characterizations. There is no significance difference in predicted performance between the two characterizations. Accordingly, the 8-component characterization was used for the remaining cross-section and 3D runs.

Grid-Size Sensitivity. Runs were made with x-direction grid dimensions from 10 to 40 and with 11 to 44 model layers. For each grid, a run was made for each of the three simulation types (rich gas, lean gas, black-oil). Table 7 lists the predicted oil recovery factor for each grid and model at the same volume of gas injected, 3000 MMscf. This is about 0.85 hydrocarbon pore volume injected for the lean gas and black-oil cases, and 0.78 HCPV for rich gas, assuming an average reservoir pressure during injection of 4000 psig. The time required to inject this volume of gas was on the order of 15 years.

Table 7 shows a slight trend of decreasing oil recovery with finer grids for black-oil model runs, but no consistent trend for the compositional model cases. Subtle trends may have been masked by a difficulty in maintaining consistent well indexes in the 2D model with changing grid size. This caused injection rates to vary somewhat for the different grid dimensions. An-other possible complicating factor is that water coning at the production well is affected by grid size. In general, however, these studies indicated that grid-size effects are small within the tested range and should not be a major factor in interpreting the 3D pattern runs.

Oil Displacement Mechanisms. Fluid saturation distributions in the cross-section model runs showed that three major factors affect sweep efficiency and oil recovery: 1) Except near the injection well, oil displacement by gas is primarily in the upper part of the reservoir because of gravity segregation and the higher permeability of the upper layers. 2) Oil saturation is reduced to zero near the injection well due to miscible displacement in the case of rich gas injection, and oil vaporization in the case of lean gas injection. The zone of zero oil saturation is much larger for the miscible case. The black-oil simulations leave residual oil in the swept regions. Other than this, the saturation distributions in the EOS model lean gas and the black-oil model runs were similar. 3) Oil and gas are displaced downward into the water-oil transition zone near the injection well (Fig. 7). Displaced water is produced at the production well by water coning.

3D Pattern Simulations

Should future Safah development include an expanded injection project with gas from outside sources, oil recovery will depend on gas composition, injection pattern, and injection pressure. Injection pattern affects oil recovery through areal sweep efficiency and injection/production well ratio. A high injection pressure enhances beneficial compositional effects and increases throughput.

Fig. 9 shows three pattern models: a line drive with a 1/5 injector/producer ratio, a 9-spot with a 1/3 well ratio, and a 5-spot with a 1/1 well ratio. All are based on a 62-acre well spacing. Each model covered a symmetry element of one-quarter of the pattern. There were 10 grid blocks between an injector and the nearest producer (14 for the 9-spot). This results in all models having square areal grids about 117 ft on each side. A 9-point difference formulation was used for the model calculations to reduce grid orientation effects. The 22-layer vertical grid (Fig. 7 and Table 6) was used in all runs. Well indexes, which relate the well grid-block pressure to the flowing bottomhole pressure, accounted for the corner location of wells in the grid block and the fractional nature of the wells (one-quarter or one-half). The same well indexes were used for injection and production wells. The original oil-in-place in each pattern is shown on Fig. 9.

Pattern Performance. The production performance of the three patterns was qualitatively similar, and is illustrated here for the 9-spot. Oil recovery differences due to pattern type are shown later. Fig. 10 shows the 9-spot cumulative production, oil rate, and GOR versus time for rich and lean gas injection. Rich gas injection recovers 1700 MSTB (10% of OOIP) more oil at 20 years than lean gas injection. Producing GOR is also significantly lower. However, with rich gas injection the “kick” in oil production rate does not occur until after five years of injection. This is unfavorable to economics should a large initial investment be needed for a miscible project. Although not shown on Fig. 10, the pattern water cut increased to 20% for rich gas injection, and to about 30% for lean gas injection, due to production of bottom water displaced by injection.

Fig. 11 shows the injection and pressure performance of the 9-spot. The gas injection rate of the pattern injector began at about 5 MMscf/D for both gas compositions, dropped to 3 MMscf/D at five years, then rose as the saturation of high-mobility gas increased in the reservoir. Injection rate at 20 years was 10 MMscf/D for lean gas and 8 MMscf/D for rich gas injection. The average pressure in the 9-spot pattern increased from 2500 psia initially, peaked near 4000 psia at five years, then slowly decreased to about 3500 psia at 20 years.

Comparison of Patterns. Fig. 12 shows the effect of pattern configuration on oil recovery. For both rich and lean gas injection, the 9-spot pattern has the highest oil recovery, followed by the line drive (except at late time). Although the 5-spot has better sweep efficiency than the line drive, its early time performance suffers because of the 1/1 injector/producer ratio. Under constant BHP injection and production constraints, maximum oil recovery *at a given time* depends on having the optimum injection/production well ratio for maximum throughput. Since gas has a much higher mobility than oil, fewer injection than production wells are needed assuming similar wellbore properties. This is an important consideration for a pattern flood operating at fixed injection and production well BHP. For Safah, it appears that the optimum well ratio is about one injection well for three producers, as in the 9-spot pattern.

Effect of Injection Pressure. High injection pressure increases pattern average pressure, which enhances compositional effects leading to increased oil recovery. Depending on facilities and gas supply, it might not be possible to inject at bottomhole pressures as high as 4500 psia. A lower injection pressure would decrease oil recovery due to: 1) reduced compositional effects, and 2) lower gas injection rate, resulting in less total gas injected at a given time.

The 5-spot pattern was used to evaluate lower injection well BHP, while maintaining the production well BHP at 1000 psia. Figs. 13 and 14 compare the 5-spot production performance for injection pressures of 4500 psia and 3000 psia. The pattern average pressure varied during the 20-year simulation, but averaged about 4200 psi for the higher and 2800 psi for the lower injection pressure. As seen on Fig. 13, 20-year recovery in a rich gas flood drops from 42% OOIP at the high injection pressure to 22% OOIP at the low injection pressure. Recovery for lean gas injection also drops significantly. (The black-oil model results are discussed below.) At the lower injection pressure, 20-year recovery for rich gas injection is only slightly more than with lean gas. As seen on Fig. 14, however, the producing GOR for rich gas injection remains significantly lower than for lean gas, indicating that some miscible or near-miscible displacement still takes place at the lower injection pressure. Because of the lower injection rate at 3000 psia injection pressure, 20 years is not sufficient time to show significant increased oil recovery from rich gas injection.

Black-Oil Modeling. Fig. 13 shows that the EOS model with lean gas injection predicts higher oil recovery than the corresponding black-oil simulation. With 4500 psia injection pressure, the increased recovery at 20 years is about 5% OOIP. This increased oil recovery is due to: 1) in the EOS model, oil vaporization near the injection well improves recovery; and 2) gas injectivity is higher in the EOS model because of the reduced oil saturation at the injector. At 3000 psia injection pressure, oil vaporization is greatly reduced; both the EOS model with lean gas injection and the black-oil model predict nearly the same oil production (Fig. 13) and GOR (Fig. 14).

In the present Safah injection project, injection wells are relatively widely spaced and average reservoir pressure is less than 3000 psia. Therefore, black-oil simulation is adequate unless reservoir pressure is increased in the future by pattern gas injection.

Produced Oil and Gas Properties. Compositional effects in a high-pressure gas injection project can be approximately monitored through produced oil and gas properties. Fig. 15 shows the GOR and separator oil and gas gravities for the producing well nearest the injector in the line drive pattern. After gas breakthrough, oil gravity increases substantially for a rich gas miscible project, and gas gravity also increases. For lean gas injection, oil gravity increases slightly, then decreases. Gas gravity gradually decreases to that of the injected lean gas.

Slug and Water Injection. Model runs were also made to investigate slug injection with various combinations of rich gas, lean gas, and water. In the 9-spot pattern, a 3-year slug of rich gas followed by lean gas recovered 42% OOIP in 20 years, compared to 49% for continuous rich gas injection and 39% for continuous lean gas injection. Combinations of water and gas injection had greatly reduced recovery at 20 years. Although water injection should improve sweep efficiency, water injectivity is extremely low because of the low Safah reservoir permeability.

Conclusions

1. Methods are presented for using laboratory PVT data, simulated PVT experiments using a cubic equation of state, and compositional reservoir simulation for evaluating miscible and immiscible gas injection. These methods can assist in the selection of laboratory PVT and displacement data, help establish displacement mechanism(s), and provide information for optimizing project design.

2. A special procedure was used to develop a fluid characterization with only eight pseudocomponents. This pseudoized characterization proved to be as accurate as the original 15-component characterization for describing standard PVT behavior, near-critical behavior, and combined vaporization/condensation effects associated with developed miscibility mechanisms.

3. Miscible displacement of Safah oil with rich gas injection could recover significantly more oil than lean gas injection. However, producing wells take over 5 years to show increased oil rates from miscible flooding, a delay which obviously is detrimental to the economics of an enriched gas miscible flood.

4. Further work is needed to optimize the level of enrichment to achieve miscible displacement at reservoir conditions developed in a BHP-controlled injection/production operation. It appears that the minimum miscibility enrichment may be less than what was used in this study.

5. In a Safah lean- or rich-gas injection project not limited by gas supply or compression capacity, the highest oil recovery at a given time is obtained with one injection well for every three producing wells.

6. Standard black-oil models appear adequate for simulating lean gas injection at low reservoir pressures where oil vaporization is minimal. At higher pressures, even immiscible lean gas injection may require fully compositional modeling to properly quantify strong vaporization effects.

Acknowledgment

The authors thank Occidental Petroleum, the Oman Ministry of Petroleum & Minerals, and Neste Exploration & Production for permission to publish this work. We also thank Aaron Zick for allowing us to use his unpublished multicell EOS method for determining MMP/MME.

References

1. Vadgama, U., Ellison, R. E., and Gustav, S. H.: “Safah Field: A Case History of Field Development”, paper SPE 21355 presented at the 1991 SPE Middle East Oil Show, Bahrain, November 16-19.
2. Chen, H-K.: “Performance of Horizontal Wells, Safah Field, Oman”, paper SPE 25568 presented at the 1993 SPE Middle East Oil Technical Conference & Exhibition, Bahrain, April 3-6.
3. Whitson, C. H.: "PVTx: An Equation-of-State Based Program for Simulating & Matching PVT Experiments with

Multiparameter Nonlinear Regression," Pera a/s, Trondheim, Norway (1992).
4. Reservoir Simulation Research Corporation (RSRC): "Modular Oil Reservoir Evaluation," User's Guide (1992).
5. Whitson, C. H.: "Characterizing Hydrocarbon Plus Fractions," *SPEJ* (Aug. 1983) 683-694; *Trans., AIME*, 275.
6. Whitson, C. H., Andersen, T. F., and Søreide, I.: "C7 Characterization of Related Equilibrium Fluids Using the Gamma Distribution," C7 Fraction Characterization, L. G. Chorn and G. A. Mansoori (ed.), Advances in Thermodynamics, Taylor & Francis, New York (1989) 1, 35-56.
7. Søreide, I.: "Improved Phase Behavior Predictions of Petroleum Reservoir Fluids From a Cubic Equation of State," Dr. Ing. thesis, IPT Report 1989:4, Norwegian Institute of Technology, Department of Petroleum Engineering and Applied Geophysics (1989).
8. Twu, C. H.: "An Internally Consistent Correlation for Predicting the Critical Properties and Molecular Weights of Petroleum and Coal-Tar Liquids," Fluid Phase Equilibria (1984) No. 16, 137-150.
9. Zick, A. A.: "A Combined Condensing/Vaporizing Mechanism in the Displacement of Oil by Enriched Gases," paper SPE 15493 presented at the 1986 SPE Annual Technical Conference and Exhibition, New Orleans, Oct. 5-8.
10. Luks, K. D., Turek, E. A., and Baker, L. E.: "Calculation of Minimum Miscibility Pressure," *SPERE* (Nov. 1987); *Trans., AIME*, 283.
11. Jensen, F. and Michelsen, M. L.: "Calculation of First Contact and Multiple Contact Miscibility Pressures," Fourth European Symposium on Enhanced Oil Recovery, Hamburg, Oct. 27-29 (1987).
12. Zick, A.: Personal communication (1993).
13. Metcalfe, R. S., Fussell, D. D., and Shelton, J. L.: "A Multicell Equilibrium Separation Model for the Study of Multiple Contact Miscibility in Rich Gas Drives," *SPEJ* (June 1973) 147-155; *Trans., AIME*, 255.
14. Coats, K. H.: "Simulation of Gas Condensate Reservoir Performance," *JPT* (Oct. 1985) 1870-1886.

Table 1—Average Reservoir and Oil Properties, Safah Undersaturated Oil Area

Reservoir temperature, °F	212
Initial pressure, psia	3100
Bubble point pressure, psia	2114
Oil gravity, °API	42
Formation vol. factor at BP, RB/STB	1.36*
Solution GOR at BP, Mscf/STB	0.54*
Oil viscosity at BP, cp	0.40
Water viscosity, cp	0.46
Permeability, md	5
Porosity	0.20

*Bo, Rs adjusted for separation at 130 psig, 100 °F

Table 2—Oil and Gas Compositions

15-Component Characterization (Mole Fraction)			
Component	Reservoir Oil	Lean Gas	Rich Gas
N_2	0.007	0.008	0.007
CO_2	0.006	0.015	0.013
C_1	0.334	0.840	0.639
C_2	0.050	0.091	0.111
C_3	0.055	0.036	0.103
IC_4	0.021	0.006	0.036
C_4	0.039	0.005	0.053
IC_5	0.020		0.017
C_5	0.028		0.014
C_6	0.044		0.006
C_{7+} (1)	0.096		
C_{7+} (2)	0.099		
C_{7+} (3)	0.087		
C_{7+} (4)	0.068		
C_{7+} (5)	0.046		

8-Pseudocomponent Characterization (Mole Fraction)			
Component	Reservoir Oil	Lean Gas	Rich Gas
C_1+N_2	0.341	0.848	0.646
C_2+CO_2	0.056	0.105	0.124
C_3	0.055	0.036	0.103
C_4's	0.059	0.011	0.089
C_5's+C_6	0.092		0.038
C_{7+} (1-2)	0.195		
C_{7+} (3-4)	0.155		
C_{7+} (5)	0.047		

Table 3—Component Properties and EOS Parameters, 15 Components
Modified Peng-Robinson EOS

Component	Mol. Weight	Critical Temp. (°R)	Critical Pressure (psia)	Acentric Factor	Critical Z-Factor	Specific Gravity	Vol. Trans. Shift s=c/b	EOS Constant Correction Factors Omega A	Omega B
N_2	28.01	227.3	493.0	.0450	.2916	.4700	- .19300	1.00000	1.00000
CO_2	44.01	547.6	1070.6	.2310	.2742	.5072	- .08200	1.00000	1.00000
C_1	16.04	343.0	667.8	.0115	.3039	.3300	- .16220	.99274	1.01049
C_2	30.07	549.8	707.8	.0908	.2898	.4500	- .11373	1.00000	1.00000
C_3	44.10	665.7	616.3	.1454	.2824	.5077	- .09094	1.00000	1.00000
IC_4	58.12	734.7	529.1	.1756	.2826	.5631	- .08894	1.00000	1.00000
C_4	58.12	765.3	550.7	.1928	.2738	.5844	- .07186	1.00000	1.00000
IC_5	72.15	828.8	490.4	.2273	.2701	.6247	- .06583	1.00000	1.00000
C_5	72.15	845.4	488.6	.2510	.2659	.6310	- .04373	1.00000	1.00000
C_6	86.18	913.4	436.9	.2957	.2708	.6640	- .01259	1.00000	1.00000
C_{7+} (1)	106.04	1026.1	409.0	.3201	.2697	.7385	.04289	.99992	1.00350
C_{7+} (2)	138.92	1141.1	352.9	.4007	.2642	.7860	.05721	.99984	1.00464
C_{7+} (3)	201.35	1300.6	274.3	.5600	.2801	.8354	.09615	.99984	1.00574
C_{7+} (4)	301.14	1471.1	206.5	.7825	.2655	.8814	.12086	.99975	1.01306
C_{7+} (5)	460.00	1645.7	158.2	1.0468	.2440	.9268	.10953	.99975	1.01306

Binary Interaction Parameters									
Component	N_2	CO_2	C_1	C_2	C_3	IC_4	C_4	IC_5	C_6 to C_{7+} (4)
CO_2	0.0								
C_1	.02500	.10500							
C_2	.01000	.13000	0.0						
C_3	.09000	.12500	0.0	0.0					
IC_4	.09500	.12000	0.0	0.0	0.0				
C_4	.09500	.11500	0.0	0.0	0.0	0.0			
IC_5	.10000	.11500	0.0	0.0	0.0	0.0	0.0		
C_5	.11000	.11500	0.0	0.0	0.0	0.0	0.0	0.0	
C_6	.11000	.11500	0.0	0.0	0.0	0.0	0.0	0.0	
C_{7+} (1)	.11000	.11500	0.02016	0.0	0.0	0.0	0.0	0.0	
C_{7+} (2)	.11000	.11500	0.02626	0.0	0.0	0.0	0.0	0.0	All 0.0
C_{7+} (3)	.11000	.11500	0.03536	0.0	0.0	0.0	0.0	0.0	
C_{7+} (4)	.11000	.11500	0.04566	0.0	0.0	0.0	0.0	0.0	
C_{7+} (5)	.11000	.11500	0.05638	0.0	0.0	0.0	0.0	0.0	

Table 4—Component Properties and EOS Parameters, 8 Pseudocomponents Modified Peng-Robinson EOS

Component	Mol. Weight	Critical Temp. (°R)	Critical Pressure (psia)	Acentric Factor	Critical Z-Factor	Specific Gravity	Vol. Trans. Shift s=c/b	EOS Constant Correction Factors Omega A	Omega B
C_1+N_2	16.30	338.8	661.5	.0127	.3055	.3336	- .16278	1.00351	1.00855
C_2+CO_2	31.53	549.4	760.9	.1113	.2953	.4576	- .11146	1.01750	1.03587
C_3	44.10	665.7	616.3	.1454	.2826	.5077	- .09094	1.00000	1.00000
C_4's	58.12	754.6	543.1	.1868	.2769	.5768	- .07783	1.00229	.99748
C_5's+C_6	78.78	877.2	462.2	.2693	.2710	.6463	- .03184	.99558	.99280
C_{7+} (1-2)	122.69	1092.1	376.8	.3663	.2641	.7650	.05104	.98309	.99562
C_{7+} (3-4)	245.03	1392.3	237.8	.6797	.2718	.8595	.10951	.96443	.99911
C_{7+} (5)	460.00	1645.7	158.2	1.0468	.2370	.9268	.10953	1.00216	1.00956

Binary Interaction Parameters

Component	C_1+N_2	C_2+CO_2	C_3	C_4's	C_5's+C_6	C_{7+} (1-2)	C_{7+} (3-4)
C_2+CO_2	0.01511						
C_3	0.00326	0.01828					
C_4's	0.00344	0.01708	0.0				
C_5's+C_6	0.00391	0.01682	0.0	0.0			
C_{7+} (1-2)	0.02678	0.01682	0.0	0.0	0.0		
C_{7+} (3-4)	0.04340	0.01682	0.0	0.0	0.0	0.0	
C_{7+} (5)	0.05834	0.01682	0.0	0.0	0.0	0.0	0.0

Table 5—Minimum Miscibility Pressure (MMP), psig

	Lean Gas		Rich Gas	
	Number of Components in EOS Characterization			
Displacement Type	15	8	15	8
Vaporizing (only)	5845	5865	4525	4505
Condensing/Vaporizing	-	-	3310	3190
Slim Tube (dispersion free)	5845	5865	3310	3190
Laboratory Slim Tube	5200 (±200)		3300 (±100)	

Table 6—Reservoir and Model Layer Properties

Geologic Zones					Model Layers (22 Total)
Zone	Thickness ft	Perm. md	Porosity	Net/Gross Ratio	Number and Thickness, ft
1	25	3.60	0.21	1.00	6 of 4.17'
2	8	5.30	0.23	1.00	2 of 4'
3A	50	1.90	0.18	0.87	8 of 6.25'
3B	30	1.00	0.20	1.00	4 of 7.5'
4A - 7	60	0.28	0.16	0.51	2 of 30'

Table 7—Effect of Grid Block Size, 2-D Variable Width Cross Section

Grid (X x Z)	Oil Recovery Factor (%OOIP) at 3000 MMscf Gas Injection		
	Black-Oil Model	EOS Model Lean Gas	EOS Model Rich Gas
10 x 11	30.9	34.5	47.7
20 x 22	28.6	34.1	49.2
30 x 33	27.8	34.7	48.4
40 x 44	27.5	35.3	47.5

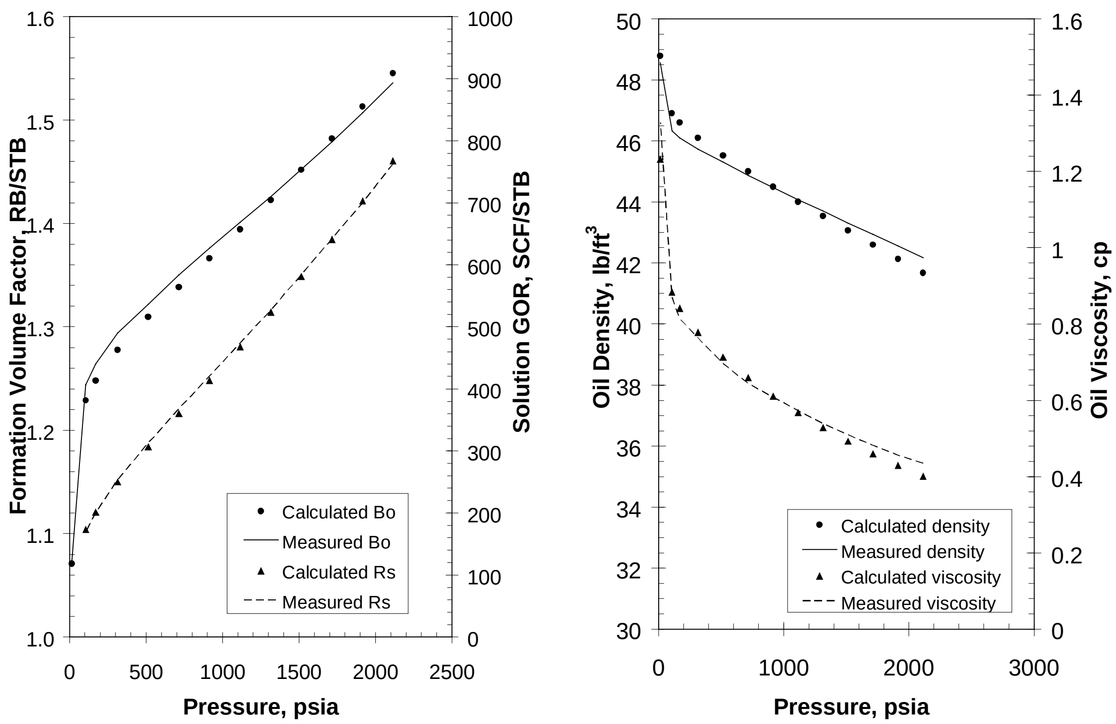

Fig. 1—Comparison of measured Safah oil PVT data with Peng-Robinson EOS match.

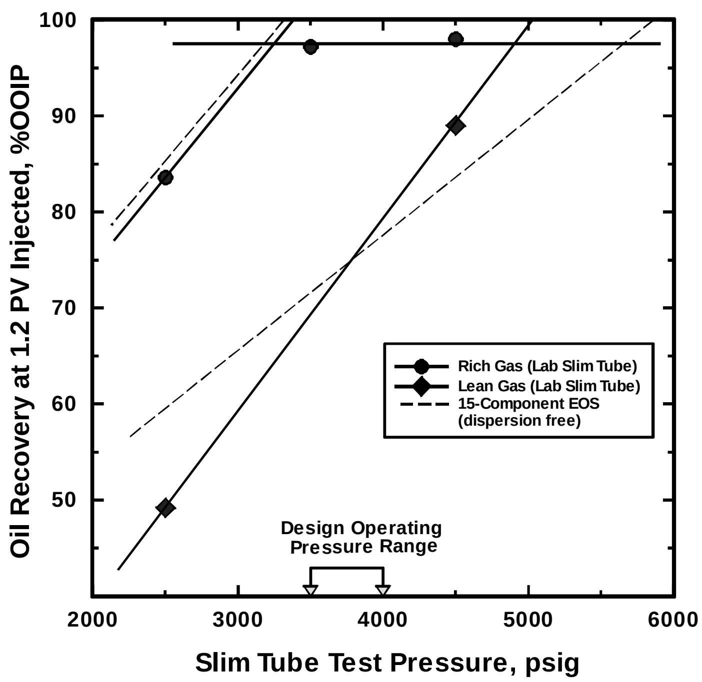

Fig. 2—Laboratory and simulated slim tube test results.

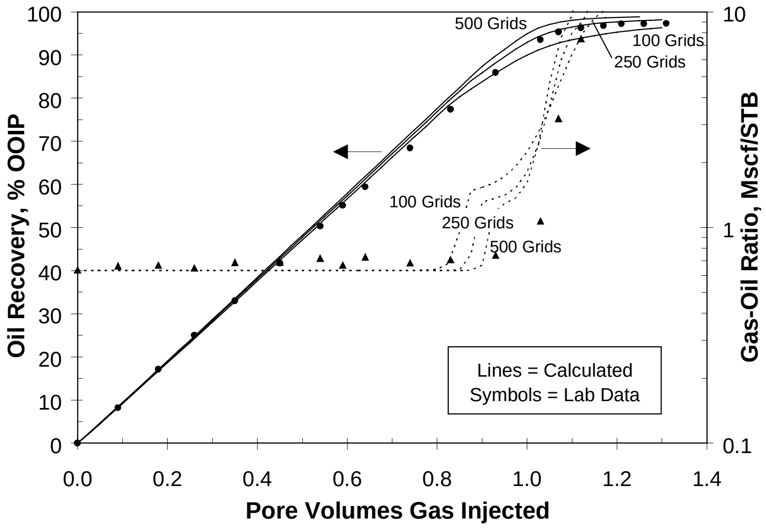

Fig. 3—Laboratory and simulated slim tube test, rich gas injection at 3500 psig.

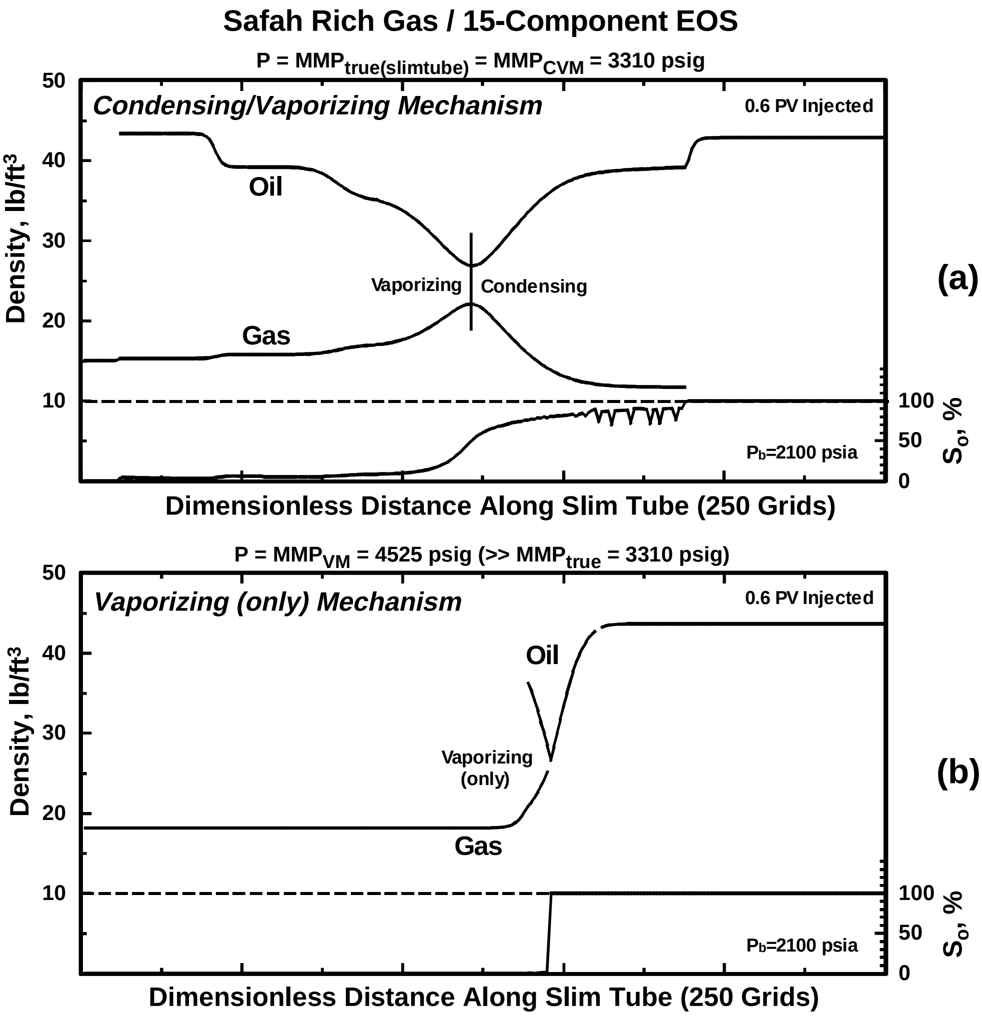

Fig. 4—Miscible slim tube simulations, rich gas injection: (a) at MMP for condensing/vaporizing mechanism; (b) at MMP for vaporizing only mechanism.

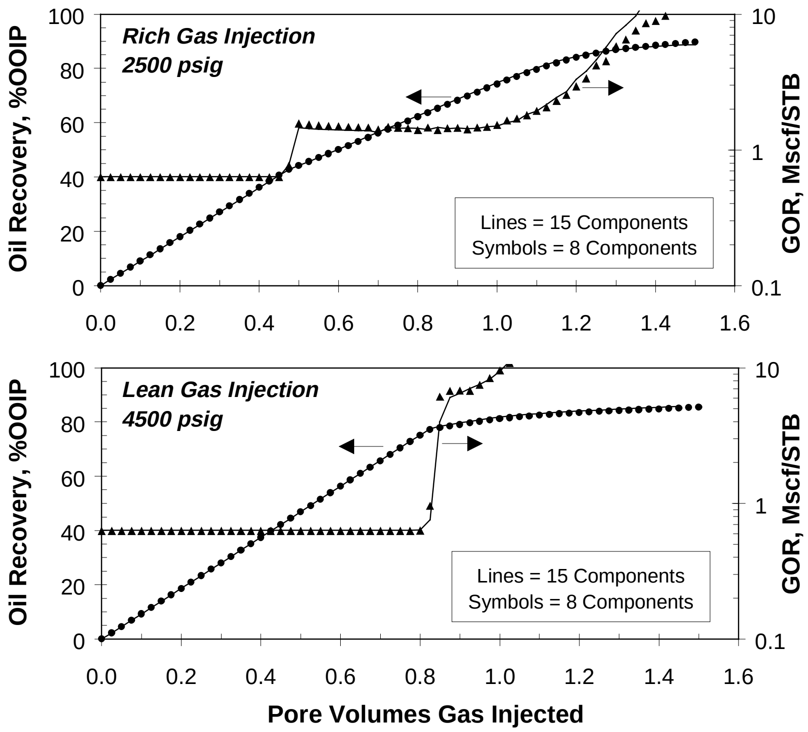

Fig. 5—Comparison of 8- and 15-component fluid characterization, simulated slim tube tests.

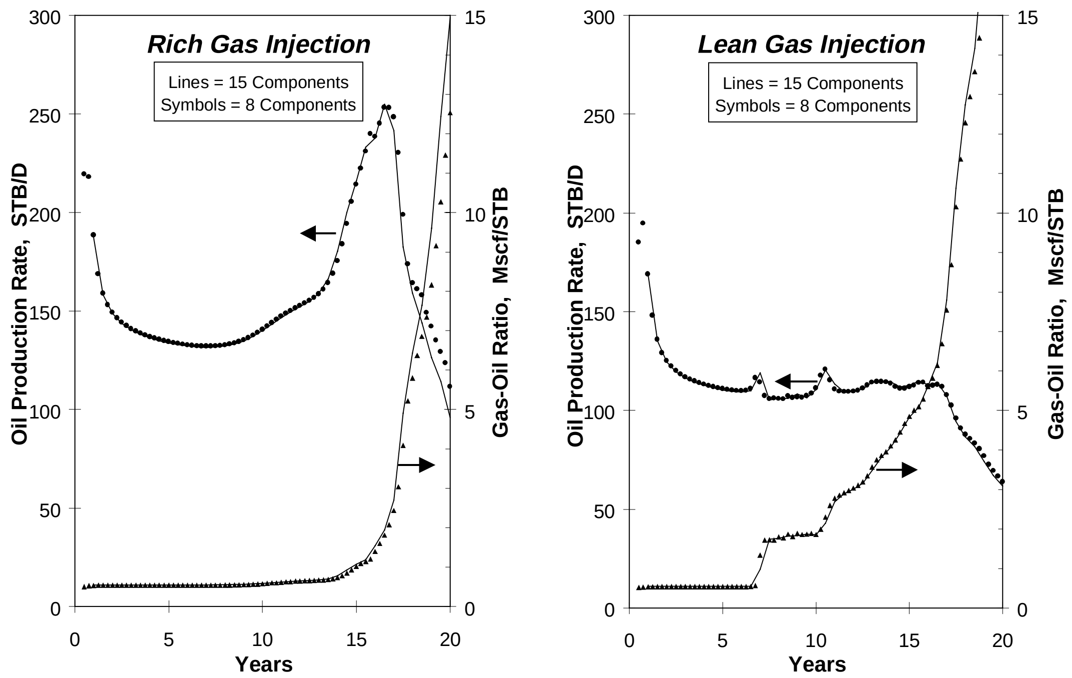

Fig. 6—Comparison of 8- and 15-component fluid characterization, 20 x 22 variable width cross section model.

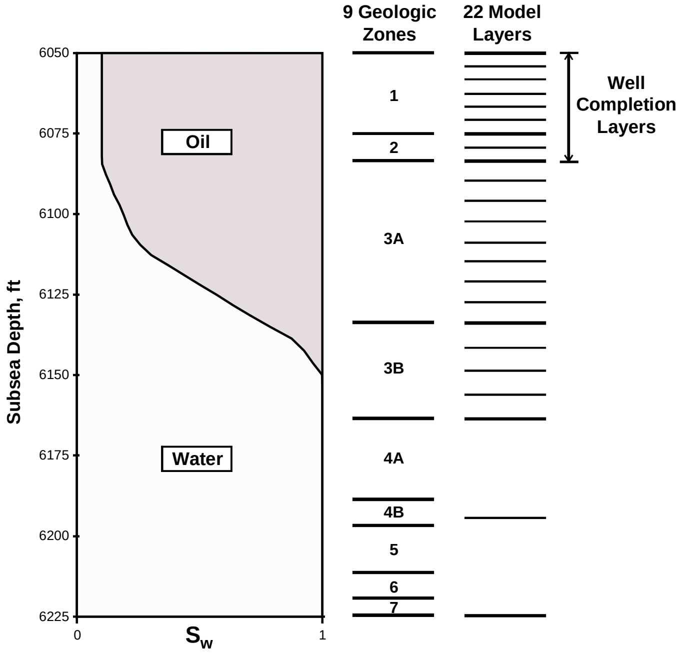

Fig. 7—Geologic zonation, vertical water/oil saturation profile, and model layers.

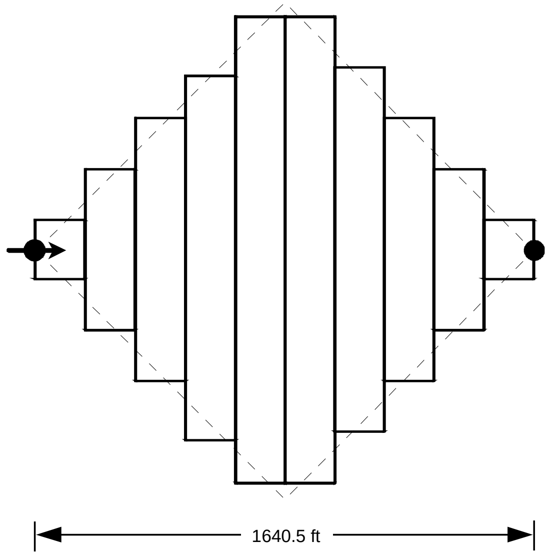

Fig. 8—2D variable width cross section model.

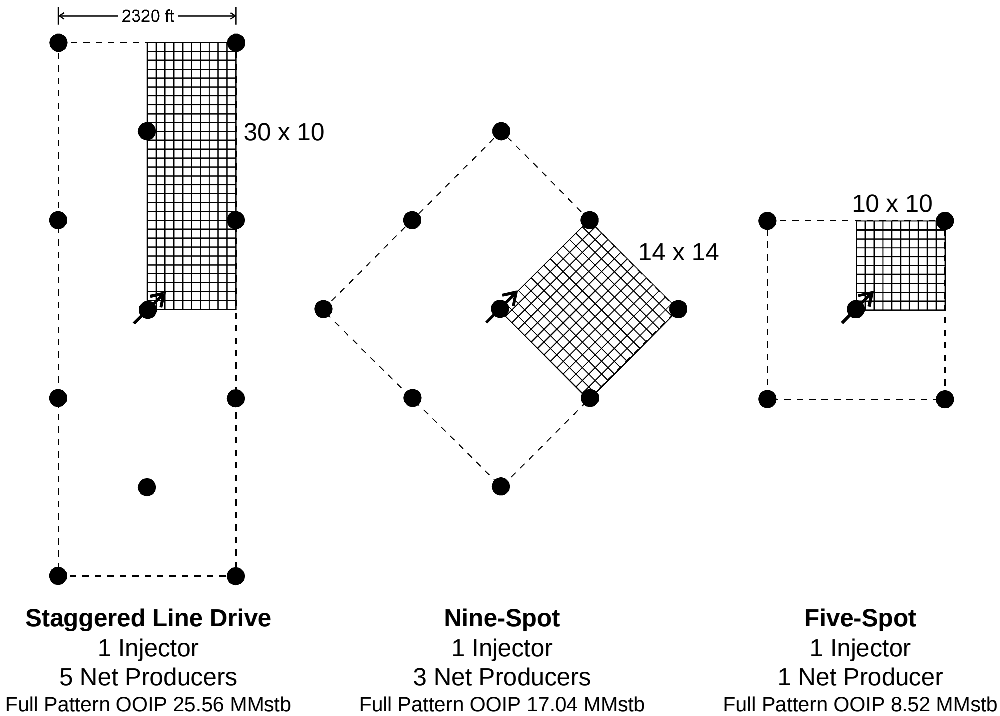

Fig. 9—3D pattern models: areal grid, well configuration, injector/producer ratio, and OOIP.

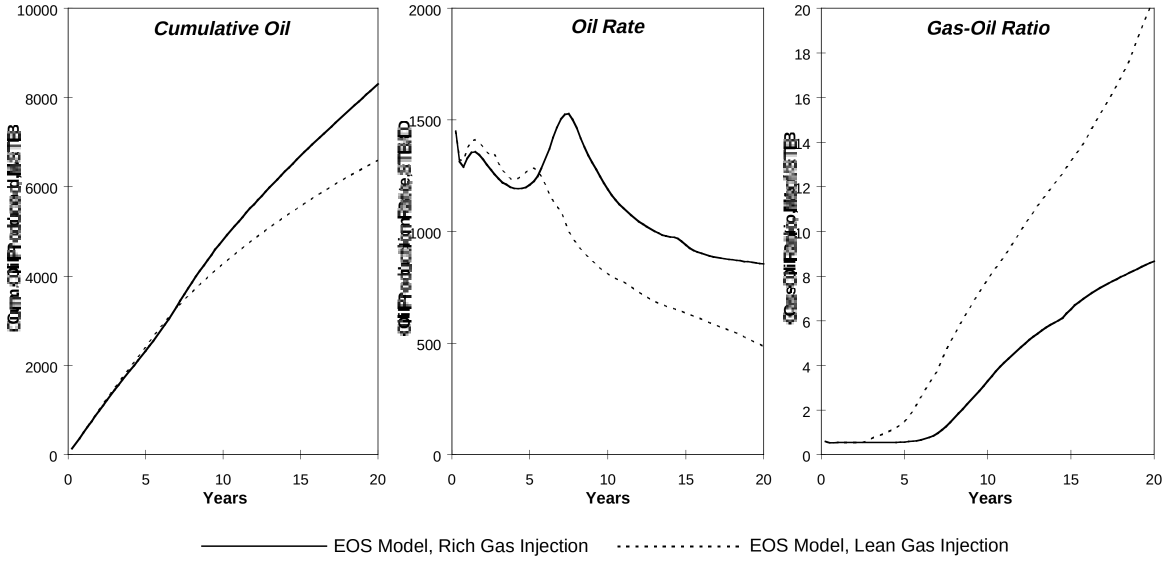

Fig. 10—Production performance of full 9-spot pattern.

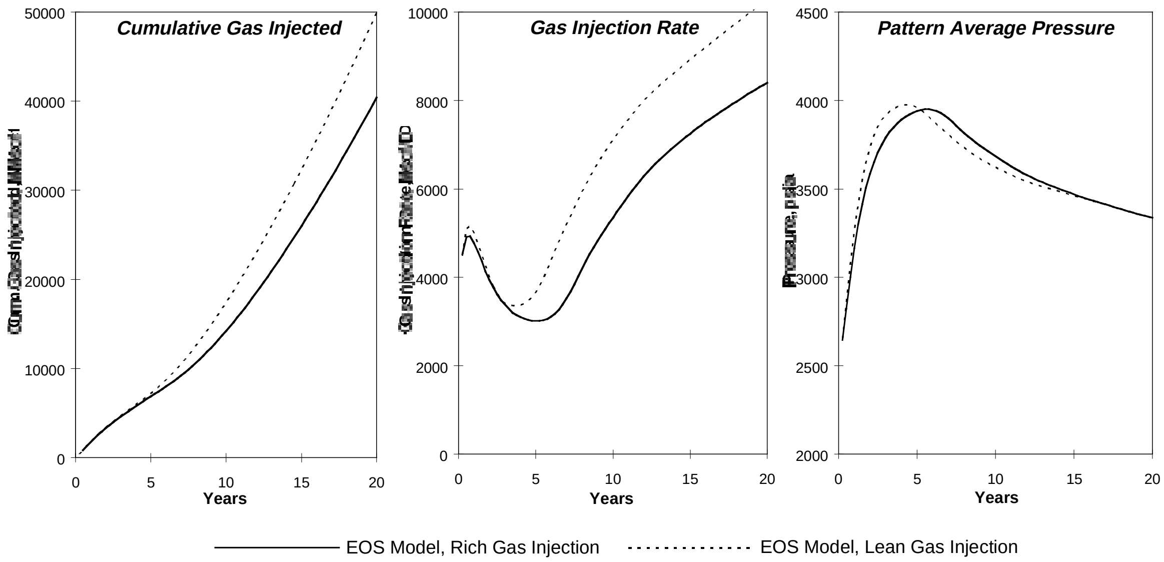

Fig. 11—Injection and pressure performance of full 9-spot pattern.

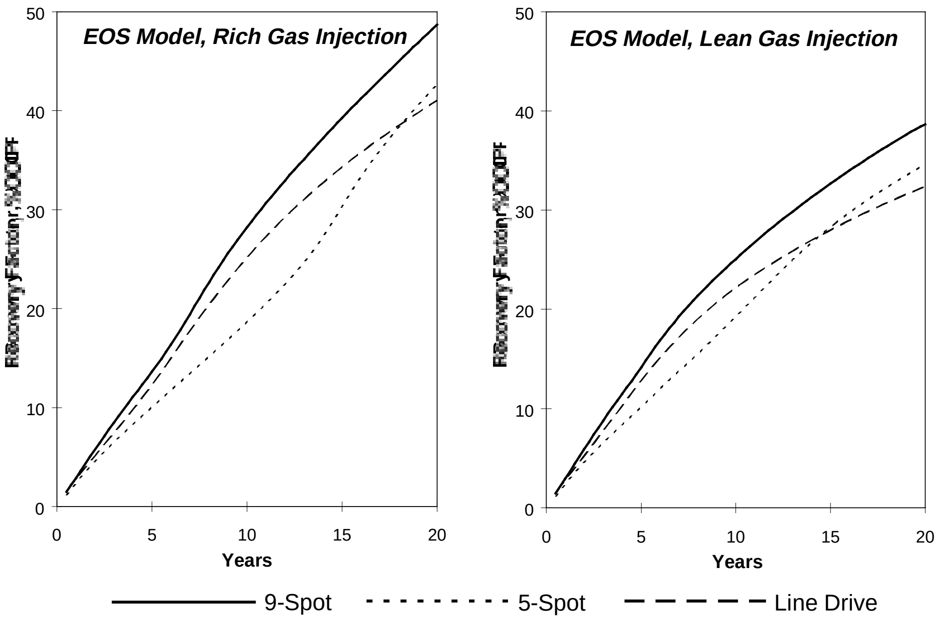

Fig. 12—Effect of pattern configuration on oil recovery.

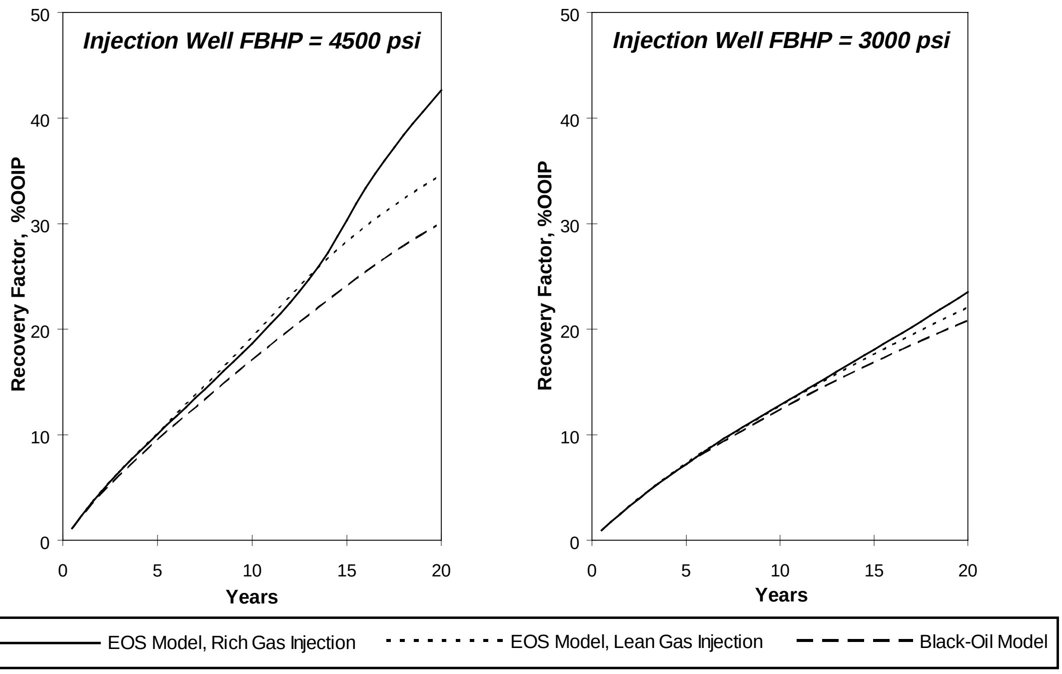

Fig. 13—Effect of injection pressure on oil recovery, 5-spot pattern.

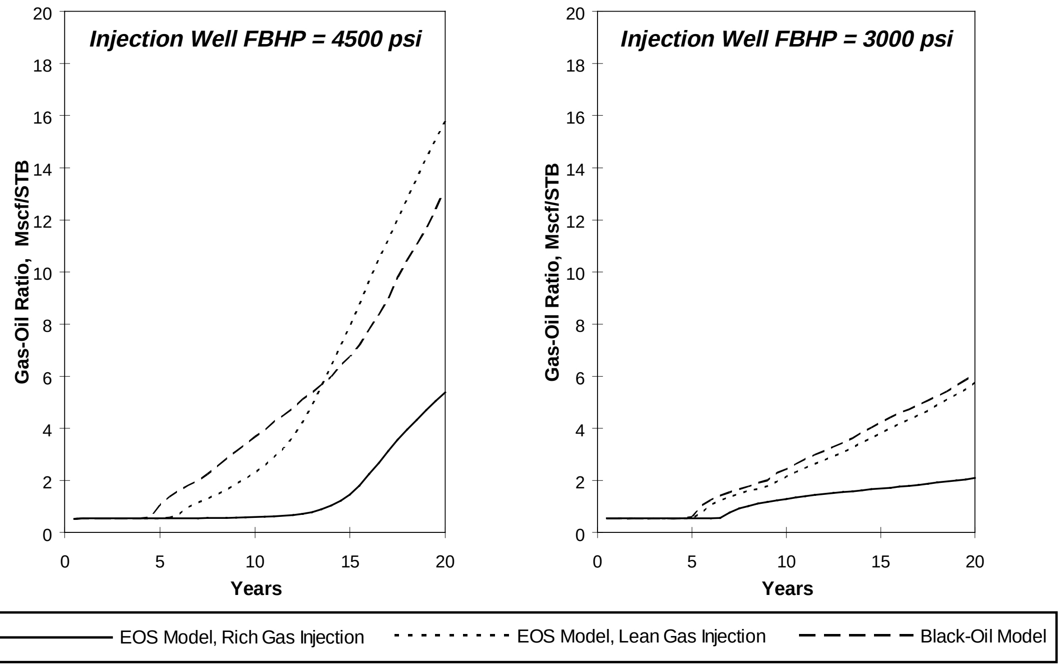

Fig. 14—Effect of injection pressure on producing gas-oil ratio, 5-spot pattern.

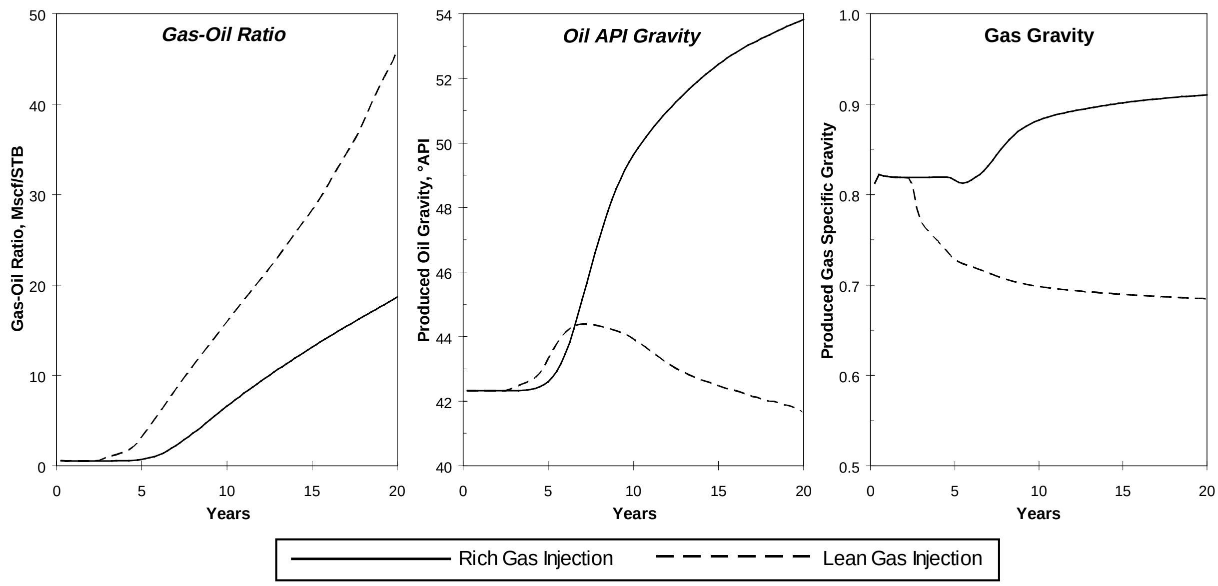

Fig. 15—Produced oil and gas properties at the nearest offset production well in the line drive pattern (separation at 130 psig, 100°F.)